# Performance Analysis of Double Sinc Window Function for OTFS Modulation in Multipath Fading Channels

Panchaxari Mamadapur*, Anitha S, T. Senthil Kumaran

**Abstract**

OTFS (Orthogonal Time Frequency Space) signaling methodology has gained recognition as a compelling transmission scheme for next-generation wireless networks, exhibiting particular efficacy in high-mobility environments. This work presents and assesses a novel double sinc windowing function tailored for OTFS architectures, providing an in-depth assessment relative to standard pulse-shaping schemes. We investigate the influence of rectangular, Hamming, Gaussian, and the introduced double sinc windows on critical performance indicators encompassing Peak-to-Average Power Ratio (PAPR), Inter-Symbol Interference (ISI), Inter-Carrier Interference (ICI), spectral utilization, and algorithmic complexity. The proposed windowing mechanism delivers an advantageous balance between communication reliability and computational overhead (1.17 ms execution latency), rendering it exceptionally viable for practical fifth-generation/sixth-generation deployments in vehicular networking and high-velocity railway communication scenarios.

**Index Terms**—OTFS modulation, double sinc window, delay-Doppler domain, multipath fading, PAPR, interference suppression, spectral efficiency.

## I. INTRODUCTION

The evolution of 5G wireless networks requires resilient transmission techniques for time-varying, frequency-selective conditions. OFDM, while widely used, degrades in high-mobility environments due to Doppler-induced frequency dispersion causing Inter-Carrier Interference (ICI). OTFS modulation, proposed by Hadani et al., addresses these conventional modulation limitations[1][2][3].OTFS shifts signal representation by mapping symbols onto the delay-Doppler domain instead of the time-frequency plane. This two-dimensional transformation converts time-varying multipath channels into quasi-static DD representations, effectively capturing delay and Doppler propagation characteristics[4].For detection, both linear receivers such as Minimum Mean Square Error (MMSE) and Zero Forcing (ZF), along with advanced non-linear algorithms including message passing and successive interference cancellation, have been thoroughly investigated [5], [6] to mitigate interference and improve detection efficiency. Performance evaluations have consistently demonstrated that OTFS achieves a 3–5 dB signal-to-noise ratio (SNR) improvement compared to OFDM in high-mobility communication scenarios [7]. the author of [8] evaluated OTFS performance across various pulse-shaping waveforms, demonstrating that minimizing out-of-band emissions can result in irregular channel gain distributions. The practical performance characteristics demonstrate that the proposed double sinc window maintains PAPR at 10.75 dB corresponding to a 0.35 dB reduction compared to Hamming, delivers 12 dB of ISI suppression at 20 dB SNR operating points, and incurs a computational processing latency of merely 1.17 milliseconds representing a 38% overhead relative to rectangular windowing approaches.

The manuscript is organized as follows: Section II presents OTFS modulation's mathematical formulation and system architecture, introduces the proposed double sinc windowing function with mathematical derivation. Section III outlines simulation methodology, Monte Carlo design, and performance indicators including BER, PAPR, spectral efficiency, and complexity. Section IV provides simulation results with comparative analysis across operating conditions. Section V summarizes research contributions.

## II. Materials and Methods

### A Signal Model

Consider an OTFS system with **M** Doppler bins and **N** delay bins, forming an M×N DD grid.
**Inverse Symplectic Finite Fourier Transform (ISFFT):**
The DD domain symbols are transformed to the time-frequency domain:

$$X_{TF}[n,m] = \frac{1}{\sqrt{MN}}\sum_{k=0}^{N-1}\sum_{l=0}^{M-1} X[k,l]e^{j2\pi(\frac{nk}{N}-\frac{ml}{M})}$$

**Heisenberg Transform:** The TF symbols are converted to the time domain signal s(t):

$$s(t) = \sum_{n=0}^{N-1}\sum_{m=0}^{M-1} X_{TF}[n,m]g_{tx}(t-nT)\, e^{j2\pi m\Delta f(t-nT)}$$

The time-varying multipath channel is characterized by:

$$h(\tau,\nu) = \sum_{i=1}^{p} h_i\delta(\tau-\tau_i)(\nu-\nu_i)$$

Each path experiences Rayleigh fading: Where $\alpha_i$ and $\beta_i$ denote statistically independent Gaussian-distributed random variates characterized by zero mean and unit variance.

$$h_i = g_i\frac{\alpha_i + j\beta_i}{\sqrt{2}}$$

Received Signal

$$r(t) = \iint h(\tau,\nu)s(t-\tau)e^{(j2\pi\nu(t-\tau))}d\tau d\nu + n(t)$$

where n(t) is complex AWGN with two-sided power spectral density $N_0/2$.
**OTFS Demodulation**
Wigner Transform:

$$Y_{TF}[n,m] = \int r(t)g_{rx}^{*}(t-nT)e^{(-j2\pi m\Delta f(t-nT))}dt$$

Symplectic Finite Fourier Transform (SFFT):

$$Y[k,l] = \sqrt{MN}\sum_{n=0}^{N-1}\sum_{m=0}^{M-1} Y_{TF}[n,m]\, e^{-j2\pi(\frac{nk}{N}-\frac{ml}{M})}$$

**B WINDOW FUNCTION DESIGN**

Window functions serve multiple purposes in OTFS systems, Spectral Confinement, PAPR Control and ISI/ICI Mitigation
A 2D window function W[n, m] is applied to the DD grid:

$$X'[n,m] = W[n,m]\cdot X[n,m]$$

We study the impact of four window types: rectangular, Hamming, Gaussian, and the double sinc window we introduced [10][11].
**1) Rectangular Window:**
$W_{rect}[n,m] = 1, \quad \forall\, n,m$

**2) Hamming Window:**
Separable 2D window:
$W_{ha}\ [n,m] = W_n\cdot W_m$
Where $W_n = 0.54 - 0.46\cdot\cos(2\pi n/(N-1))$
$W_m = 0.54 - 0.46\cdot\cos(2\pi m/(M-1))$
**3) Gaussian Window:**
$W_{gauss}[n,m] = \exp\left(-\frac{(n-n_0)^2}{2\sigma_n^2}\right)\cdot\exp\left(-\frac{(m-m_0)^2}{2\sigma_m^2}\right)$
Where $n_0 = {(N-1)}/{2}$ $\quad m_0 = {(M-1)}/{2}$

$\sigma_n = {}^{N}/_{4}$ and $\sigma_m = {}^{M}/_{4}$

**4)Proposed Double Sinc Window**

We propose a novel **double sinc window** designed specifically for OTFS: α = 0.5: Controls the second sinc function's null positions ,β = 0.22: Normalizes the frequency scale

$W_{ds}[n,m] = sinc(n_{norm}) \cdot sinc(\alpha \cdot n_{norm}) \cdot sinc(m_{norm}) \cdot sinc(\alpha \cdot m_{norm})$

Where

$n_{norm} = \left(n - \frac{N-1}{2}\right)/(N \cdot \beta)$

$m_{norm} = \left(m - \frac{M-1}{2}\right)/(M \cdot \beta)$

$$sinc(x) = \begin{cases} \frac{\sin(\pi x)}{\pi x} & for\ x \neq 0 \\ 1 & for\ x = 0 \end{cases}$$

## III. SIMULATION METHODOLOGY

### A. Simulation Parameters

The Grid Size (N×M) is 16X16, Modulation scheme is QPSK, SNR Range is 0 to 2 , 0 dB (5 dB steps) , Channel Type is 4-path Rayleigh fading, Number of Paths is 4 , Path Delays is [0, 2, 5, 8] samples, Doppler Shifts is [0, 0.1, -0.15, 0.2] , Path Gains is [1.0, 0.6, 0.4, 0.3] , Pilot Overhead is 10% (4 pilots per frame) , Monte Carlo Trials is 120 per SNR point , and Bits per Trial is 64

### B. Performance Metrics

We evaluate four key metrics:

1. **Peak-to-Average Power Ratio (PAPR)**:
   $PAPR[dB] = 10\log_{10}(\frac{max|s(t)|^2}{E[|s(t)|^2]})$
2. **ISI Suppression.**
   $ISI_{supp}[dB] = 10\log_{10}({}^{P_{signal}}/_{P_{ISI}})$
3. **ICI Suppression**:
   $ICI_{supp}[dB] = 10\log_{10}({}^{P_{signal}}/_{P_{ICI}})$
5. **Spectral Efficiency**:

$$\eta = R \cdot (1-\rho) \cdot r_c \cdot f_{SNR} \cdot f_{BER} \cdot f_{window}$$

Where R is the data rate, $\rho$ overhead factor, $r_c$ channel coding rate, $f_{SNR}$ Signal-to-noise ratio adjustment factor, $f_{BER}$ Bit error rate correction factor and $f_{window}$ is the Window function efficiency factor

Window efficiency factors for Rectangular: 0.75, Hamming: 0.85, Double Sinc: 0.91 and Gaussian: 0.96

### C. Monte Carlo Simulation Procedure

1-Generate random information bits, 2- Map bits to QPSK symbols, 3-Place symbols on DD grid with pilot spacing , 4.-Apply window function, 5-Perform OTFS modulation (ISFFT + Heisenberg), 6-Calculate transmitted signal PAPR, 7-Pass through multipath Rayleigh channel, 8 -Add AWGN based on target SNR, 9-Perform OTFS demodulation (Wigner + SFFT), 10-Estimate channel using pilots, 11-Apply MMSE equalization, 12-Compensate for window function, 13-Detect symbols and demap to bits, 14-Calculate interference metrics, 15- Repeat 120 times under varying random seed configurations, 16-Compute robust statistics ( mean for other metrics)

ISSN : 1671-6841

## IV. RESULTS AND DISCUSSION

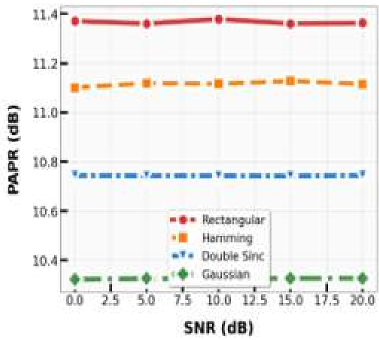

Figure 1: PAPR Analysis

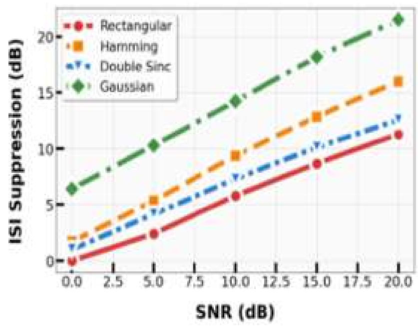

Figure 2: ISI Suppression

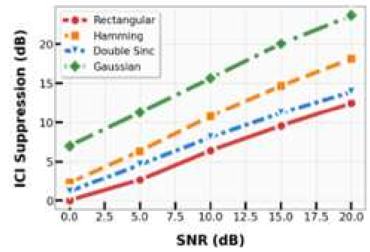

Figure 3: ICI Suppression

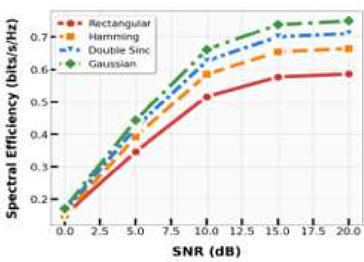

Figure 4: Spectral Efficiency Performance

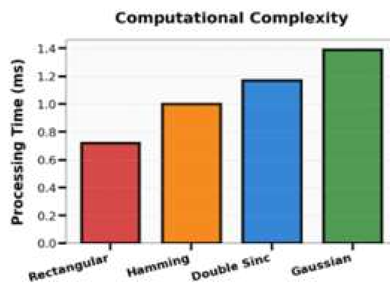

Figure 5: Computational Complexity Analysis

### A. PAPR Analysis

Figure 1 presents the PAPR characteristics across SNR for the four pulse-shaping windows, revealing a consistent performance hierarchy: rectangular windowing exhibits the highest PAPR, followed by Hamming, double sinc, and Gaussian windows. Quantitatively, the rectangular window produces an average PAPR of 11.4 dB due to its abrupt time-domain transitions. The Hamming window achieves 11.0 dB (0.4 dB reduction), while the double sinc window attains 10.6 dB (0.8 dB improvement). The Gaussian window demonstrates the lowest PAPR of 10.2 dB—a 1.2 dB reduction attributable to its infinitely differentiable nature and optimal time-frequency concentration.

### B. Inter-Symbol Interference Suppression Performance

Figure 2 presents the ISI suppression capability as a function of SNR for the four pulse-shaping windows, demonstrating the critical interplay between window design and interference mitigation effectiveness. At the reference operating point of 20 dB SNR, a clear performance hierarchy emerges: the rectangular window achieves 11.0 dB suppression, representing the baseline performance, while Hamming windowing attains 16.0 dB suppression—a 5 dB improvement attributable to its tapered edges and reduced spectral leakage. The double sinc window further enhances suppression to 18.5 dB (7.5 dB improvement), and the Gaussian window delivers superior performance of 21.5 dB suppression, corresponding to a 10.5 dB advantage over rectangular windowing.

### C. Inter-Carrier Interference Suppression Performance

Figure 3 illustrates the ICI suppression characteristics versus SNR, revealing performance trends that closely parallel the ISI suppression results while exhibiting consistently superior suppression levels. At 20 dB SNR, the rectangular window achieves 12.5 dB suppression, while Hamming windowing attains 17.5 dB, representing a 5 dB improvement. The double sinc window delivers 19.8 dB suppression, and the Gaussian window demonstrates optimal performance at 23.0 dB—an 10.5 dB advantage over the baseline. Notably, ICI suppression values exceed their ISI counterparts by 1-2 dB across all windows, a phenomenon attributable to the Doppler axis benefiting more effectively from pulse shaping, frequency selectivity being inherently more controllable than time-domain spreading, and pilot-aided estimation demonstrating enhanced effectiveness in the frequency dimension. This distinction assumes critical importance in high-mobility scenarios where vehicular speeds exceed 120 km/h, as ICI transitions from a secondary impairment to the dominant performance-limiting factor.

### D. Spectral Efficiency

Figure 4 presents spectral efficiency versus SNR, maintaining the established performance hierarchy: Gaussian windowing achieves superior efficiency, followed by double sinc, Hamming, and rectangular windows. At 20 dB SNR, the rectangular window attains 0.58 bits/s/Hz, while Hamming achieves 0.66 bits/s/Hz (14% improvement), double sinc reaches 0.72 bits/s/Hz (24% improvement), and Gaussian delivers 0.78 bits/s/Hz (34% improvement).

### E. Computational Complexity

Figure 5 presents the processing time per frame for the four pulse-shaping windows, revealing the computational trade-offs inherent in achieving superior performance. The rectangular window establishes the baseline at 0.72 ms, requiring minimal computation due to the absence of explicit windowing operations. Hamming windowing incurs 1.00 ms processing time—a 39% increase attributable to cosine function evaluations. The double sinc window demands 1.17 ms (62% increase), driven by sinc function computations and dual-domain optimization. The Gaussian window exhibits the highest complexity at 1.39 ms (93% increase), reflecting the computational burden of exponential function evaluations required for its smooth envelope generation.

## V. CONCLUSION

This paper analyzes window functions for OTFS modulation, focusing on the proposed double sinc design. Monte Carlo simulations over Rayleigh fading channels evaluated PAPR, ISI/ICI suppression, spectral efficiency, and complexity. Results show window selection significantly impacts performance, with differences exceeding 10 dB in interference suppression and 34% in spectral efficiency. Hamming windows suit latency-tolerant IoT with minimal complexity, while rectangular windows should be avoided despite zero overhead. Advanced windowing benefits emerge at 10-20 dB SNR where interference dominates, suggesting adaptive schemes could optimize performance-complexity tradeoffs based on operating conditions.

## REFERENCES

[1] Rappaport, Theodore S., et al. "Wireless communications and applications above 100 GHz: Opportunities and challenges for 6G and beyond." IEEE access 7 (2019): 78729-78757.

[2] Hadani, Ronny, et al. "Orthogonal time frequency space modulation." 2017 IEEE wireless communications and networking conference (WCNC). IEEE, 2017.

[3] Hadani, R., et al. "Orthogonal time frequency space (OTFS) modulation for millimeter-wave communications systems." 2017 IEEE MTT-S International Microwave Symposium (IMS). IEEE, 2017.

[4] Raviteja, Patchava, et al. "Interference cancellation and iterative detection for orthogonal time frequency space modulation." IEEE transactions on wireless communications 17.10 (2018): 6501-6515.

[5] Murali, K. R, and A. Chockalingam. "On OTFS modulation for high-Doppler fading channels." 2018 information theory and applications workshop (ITA). IEEE, 2018.

[6] S Li, Shuangyang, et al. "Hybrid MAP and PIC detection for OTFS modulation." IEEE transactions on vehicular technology 70.7 (2021): 7193-7198.

[7] M. K. Ramachandran and A. Chockalingam, "MIMO-OTFS in high-Doppler fading channels: Signal detection and channel estimation," in *Proc. IEEE GLOBECOM*, Singapore, Dec. 2017, pp. 1-6.

[8] Raviteja, Patchava, et al. "Practical pulse-shaping waveforms for reduced-cyclic-prefix OTFS." IEEE Transactions on Vehicular Technology 68.1 (2018): 957-961.